IJWA

An Advanced Method for Iris Segmentation and Normalization

Mahboubeh Shamsi[1], Abdolreza Rasouli[2], Puteh Bt Saad[3], Soudeh Shadravan[4]
[1, 2, 4] Faculty of Computer Science & Information System Islamic Azad University
Bardsir, Iran
mahboubehshamsi@yahoo.com[1], rs.reza@gmail.com[2], shadra239@yahoo.com[4]
[3] Faculty of Computer Science & Information System University Technology of Malaysia (UTM)
Skudai, Malaysia
drputeh@gmail.com[3]

ABSTRACT: *Iris is a desirable biometric representation of an individual for security-related applications. However the iris segmentation and normalization process is challenging due to the presence of eye lashes that occlude the iris, the dilation of pupils due to different light illumination and several other uncontrolled factors. In this work, we enhanced Daugman method to locate the iris and normalized it from Polar to Cartesian coordinate. The algorithm is tested using iris images from CASIA database and MMU database. The percentage detection on MMU iris database is 99% and that of CASIA is 98%. Our approach is feasible to produce an iris template for identity identification and biometric watermarking application.*

Keywords: Iris Recognition, Biometric Identification, Recognition, Automatic Segmentation.

Received: 15 August 2009, Revised 21 September 2009, Accepted 15 October 2009

1. Introduction

Enterprises are now global, virtual and dependent on dynamic information access. By nature, digital information is in constant motion throughout its lifecycle. In this shifting landscape, the battlefront in security is rapidly changing from securing the perimeter to protecting the information itself. A biometric system provides automatic recognition of an individual based on a unique feature possessed by an individual. Biometric systems have been developed based on fingerprints, facial features, voice, hand geometry, handwriting, the retina (Sanderson and Erbetta 2000), and the one presented in this paper, the iris.

The first phase of iris Biometric systems is capturing the sample of the iris. Then iris samples are preprocessed and segmented to locate the iris. Once the iris is located, it is then normalized from polar coordinate to Cartesian. Finally a template representing a set of features from the iris is generated. The iris template can then be objectively compared with other templates in order to determine an individual's identity. Most biometric systems allow two modes of operation. An enrolment mode for adding templates to a database, and an identification mode, where a template is created for an individual and then a match is searched from a database of pre-enrolled templates.

Iris biometric has the following desirable properties, firstly an iris image is unique, the statistical probability that two irises would be exactly the same is estimated at 1 in 1072 (Williams 2001). Two different irises are extremely unlike to be equal, even in the case of genetically identical twins (Daugman 2002). Secondly, the iris is stable and reliable since it does not vary with age and no foreign material can contaminate the iris, contact lens or spectacle do not hinder the capturing of the iris. Thirdly the iris fulfills the aliveness check (contraction of the pupil in response to light), where an imposter is unable to provide a fake iris image and finally it can be easily captured.

This paper is expected to contribute towards the algorithm for Iris recognition continues to will be acknowledged as the most accurate biometric identification system available in the world today.

In the commercial systems iris biometric applications are used to such as computer network login, electronic data security, ecommerce, Internet access, ATM, credit card, physical access control, cellular phone, PDA, medical records management, distance learning. It also could be used to such as national ID card, correctional facility, driver's license, social security, welfare-disbursement, border control, passport control. There are also so many applications that use biometric systems for

protecting privacy information that can implement by this algorithm safely in the real world. This paper has been organized in five sections. First section will continue on basic information about iris structure. Then, the main steps of iris recognition will be described. Section two has been divided to two parts. First part is a background on iris segmentation and second part has been committed to our segmentation algorithm. Section three is assigned to our normalization algorithm. The paper will be continued on our earned result on section four and will be ended with discussion and conclusion.

1.1 The Human Iris

The thin circular diaphragm, which separate between the cornea and the lens of the human eye is iris. The iris is perforated close to its centre by a circular aperture known as the pupil. The sphincter and the dilator muscles, which adjust the size of the pupil, can control the light entering through the pupil. The average diameter of the iris is 12 mm (Daugman 2002). The iris consists of layers, the epithelium layer and the stroma layer. The epithelium layer contains dense pigmentation cells. The stroma layer that lies above the epithelium layer contains blood vessels, pigment cells and two iris muscles.

The color of the iris, depend to density of stroma pigmentation determines. The surface of the multi-layered iris that is visible includes two sectors that are different in color (Wolff 1976), an outer ciliary part and an inner pupillary part. These two parts are divided by the collarette – which appears as a zigzag pattern. The iris is formatted of the third month of embryonic life (Wolff 1976). In during the first year of life the unique pattern on the surface of the iris is formed. Formation of the unique patterns of the iris is random and not related to any genetic factors (Wildes 1997). But the pigmentation of the iris is dependent on genetics. This is only and one character that depend on genetics. Also this character determines the color of it. Due to the epigenetic nature of iris patterns, the two eyes of an individual contain completely independent iris patterns, and identical twins possess uncorrelated iris patterns (Wolff 1976).

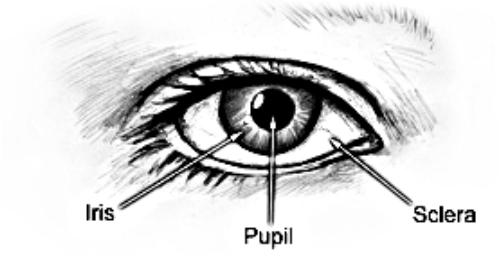

Figure 1. Human eye components

1.2 Iris Recognition

Figure 2 illustrated steps of recognize an iris from the eye's image. In Iris Acquisition the eye image is captured. In Segmentation, the iris region in an eye image is located. A dimensionally consistent representation of the iris region is created in the normalization step. Finally a template containing only the most discriminating features of the iris is generated in the feature encoding stage.

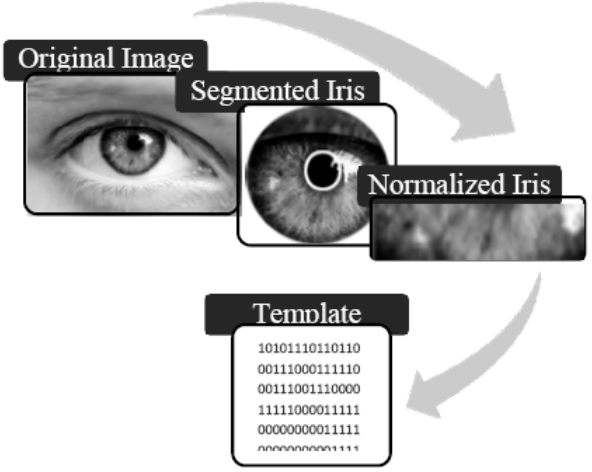

Figure 2. Iris Recognition Process

2. Segmentation

In segmentation two circles are utilized to separate between iris/sclera boundary and iris/pupil boundary. The eyelids and eyelashes normally occlude the upper and lower parts of the iris region.

The success of a segmentation process depends on the imaging quality of eye images . An individual with darkly pigmented irises display a low contrast between the pupil and iris region if the image is acquired under natural light, making segmentation more difficult (Barry and N.). An automatic segmentation algorithm based on the circular Hough transform is employed by Wildes et al. (Wildes, et al. 2004), Kong and Zhang (Kong and Zhang 2001), Tisse et al. (Tisse, et al. 2002), and Ma et al. (Ma, et al. 2002). These parameters are the centre coordinates xc and yc, and the radius r, which are able to define any circle according to the equation:

$$x_c^2 + y_c^2 - r^2 = 0$$

Wildes et al. (Wildes, Asmuth, Green and Hsu 2004) and Kong and Zhang (Kong and Zhang 2001) also make use of the parabolic Hough transform to detect the eyelids, approximating the upper and lower eyelids with parabolic arcs, which are represented as:

$$(-(x-h_j)\sin\theta_j + (y-k_j)\cos\theta_j)^2 = a_j((x-h_j)\cos\theta_j + (y-k_j)\sin\theta_j)$$

Where the aj controls the curvature, the peak of the parabola is (hj, kj) and the angle of rotation relative to the x- axis is θj.

Daugman (Daugman 2002) makes use of differential operator for locating the circular iris and pupil regions, and also the arcs of the upper and lower eyelids. The differential operator is defined as

$$\max_{(r, x_p, y_o)} \left| G_\delta(r) * \frac{\partial}{\partial_r} \oint_{r, x_o, y_o} \frac{I(x,y)}{2\pi r} d_s \right|$$

The eye image is I(x, y), the radius should be looked for is r, the Gaussian smoothing function is Gδ(r) and s is the contour of the circle given by r, x0, y0. The operator searches for the circular path where there is maximum change in pixel values, by varying the radius and centre x and y position of the circular contour.

Ritter et al. (Ritter 1999) make use of active contour models for localizing the pupil in eye images. Pre-set internal and external forces are responded with active contours. Now active contours respond by deforming internally or moving across an image. This process continues until equilibrium is reached. The contour includes some vertex. These vertices have positions that are changed by two opposing forces:

1. An internal force: It depends on the desired characteristics
2. An external force: It depends on the image

Each vertex is moved between t and t+1 by

$$V_i(t+1) = V_i(t) + F_i(t) + G_i(t)$$

The internal force is Fi, the external force is Gi and the position of vertex i is Vi. For localization of the pupil region we need two forces:

1. The internal forces: they are calibrated so that the contour forms a globally expanding discrete circle.
2. The external forces: they are usually found using the edge information.

In order to improve accuracy Ritter et al. (Ritter 1999) use the variance image, rather than the edge image. 1D Gabor filters is useful for detecting separable eyelashes. Another model is The Kong and Zhang model (Kong and Zhang 2001). They also make use of connective criterion, so that each eyelash's point must connect to another eyelash's point or eyelid's point. Wildes et al (Wildes, Asmuth, Green and Hsu 2004) suggested the vertical direction with Gradients for the outer iris/sclera boundary. For the inner iris/pupil boundary, Vertical and horizontal gradients were weighted equally. A modified version of Kovesi's Canny edge detection MATLAB function (Kovesi) was implemented, which allowed for weighting of the gradients. In order to ensure the iris detection is efficient and accurate, boundary between iris and sclera circle is detected using Hough Transform in the iris region, instead of the whole eye region, since the pupil is always within the iris region.

2.1. Iris Localization

Base on Daugman operator, Mazur (Mazur 2007) proposed a slight nonlinear modification and reformulate the operator for speeding up the computation. The form is:

$$\max_{(n\Delta r, x_o, y_o)} \left| \sum_k \{ \frac{(G_\sigma(a_0) - G_\sigma(a_1)) \sum_m I(b_x, b_y)}{\Delta r \sum_m I(c_x, c_y)} \} \right|$$

With

$$a_0 = (n - k)\Delta r,\ a_1 = (n - k - 1)\Delta r,$$
$$b_x = k\Delta r \cos(m\Delta\varphi) + x_0,$$
$$b_y = k\Delta r \sin(m\Delta\varphi) + y_0,$$
$$c_x = (k - 2)\Delta r \cos(m\Delta\varphi) + x_0,$$
$$c_y = (k - 2)\Delta r \sin(m\Delta\varphi) + y_0$$

For each (r, x0, y0) we must survey two sums over m that is in numerator and denominator and sum over k with one multiplication in numerator.

Based on Daugman method, we construct a kind of circular edge detector by using a series of accumulated images as illustrated in Figure 3.

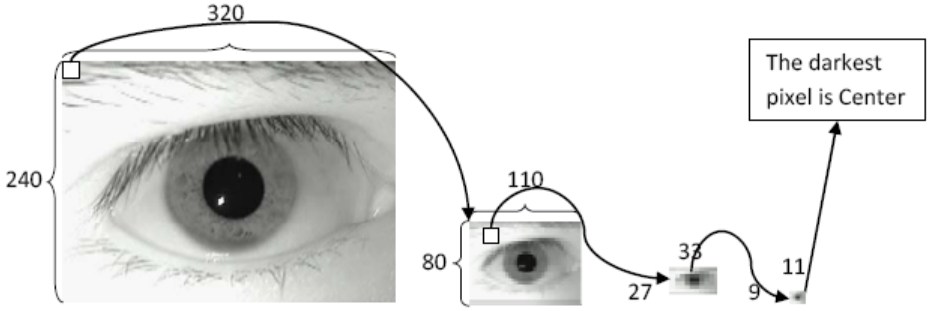

Figure 3. An example series of accumulated images

It is impossible to calculate Daugman Operator for all feasible circles of an image. Therefore, we should restrict the space of potential circles. For instance, in many researches, they assume that the center of iris is near the center of image. Also they spot a range of radius which is based on the size of image. The accumulating process has been applied for finding a potential centers and covering area. This area will be passed to Daugman Operator to find actual center of iris.

The actual center of image (center of pupil) is covered by the area of the dark pixel of the lowest resolution. But in higher resolution, this area covered by a number of pixels that is up to the relevant smoothing factor Sf. All of images are obtained from higher resolution by accumulating, except the input image I0. The follow formula is used for defining the coordinates of the point as show in Figure 4.

$$x = x_k = x_0 + [r \cos \alpha], y = y_k = y_0 + [r \sin \alpha_k]$$

That K and αk=2πk/K are the number of points taken in to integration over the circle. ΔI is used for defining by simple differences in two orthogonal directions of the input image as follows:

$$\Delta I(x_k, y_k) = I(x + \Delta_a, y + \Delta_a) - I(x - \Delta_a, y - \Delta_\alpha)\ \Delta I = I_1 + I_2 + I_3 + I_4$$
$$I_1 = (I(x_k + 1, y_k) - I(x_j - 1, y_k)) \cdot \cos(\alpha_k)$$
$$I_2 = (I(x_k, y_k + 1) - I(x_k, y_k - 1)) \cdot \sin(\alpha_k)$$
$$I_3 = (I(x_k + 1, y_k + 1) - I(x_k - 1, y_k - 1)) \cdot \sin(45 + \alpha_k)$$
$$I_4 = (I(x_k + 1, y_k - 1) - I(x_k - 1, y_k + 1)) \cdot \cos(45 + \alpha_k)$$

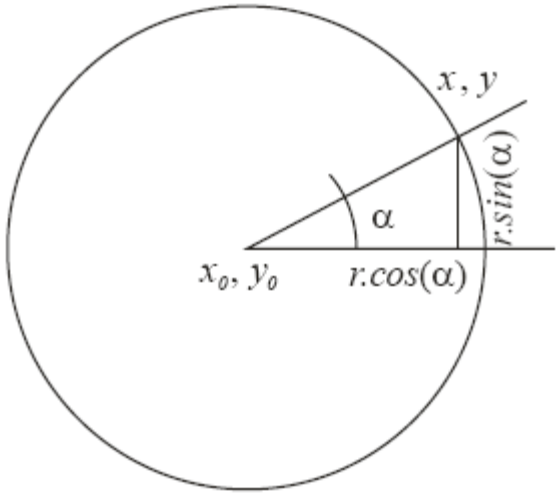

Figure 4. Defining circle's coordinates

Based on the above equations, we will describe the algorithm.

Create a series of accumulated image In using smoothing factor Sf. The minimum value of In is a center of the pupil as (x0, y0). For each accumulated image starting from more to less resolution images do these steps:

1. construct a set of potential center around the point defined by initial values obtained as the result of the previous stage

$$[x_0 \pm \frac{S_f}{2}] \times [y_0 \pm \frac{S_f}{2}]$$

2. construct a set of potential radiuses

$$[r \pm \frac{S_f}{2}]$$

3. Apply the Daugman operator and find optimal center and radius

$$\arg\max_{(r,x,y)} \sum_{k=1}^{k} \Delta I\left(x_k, y_k\right)$$

$$\forall [x, y] \in [x_0 \pm \frac{S_f}{2}] \times [y_0 \pm \frac{S_f}{2}],\ r \in [r \pm \frac{S_f}{2}]$$

$$x_k = x_0 + r \cdot \cos(\alpha_k),\ y_k = y_0 + r \cdot \sin(\alpha_k), \alpha_k = 2\pi * k/k$$

$$\Delta I\,(x_k, y_k) = I(x + \Delta_a, y + \Delta_a) - I(x - \Delta_a, y - \Delta_a)\ \Delta I = I_1 + I_2 + I_3 + I_4$$

$$I_1 = (I\,(x_k + 1, y_k) - I\,(x_j - 1, y_k)) \cdot \cos(\alpha_k)$$

$$I_2 = (I\,(x_k, y_k + 1) - I\,(x_j, y_k - 1)) \cdot \sin(\alpha_k)$$

$$I_3 = (I\,(x_k + 1, y_k + 1) - I\,(x_k - 1, y_k - 1)) \cdot \sin(45 + \alpha_k)$$

$$I_4 = (I\,(x_k + 1, y_k - 1) - I(x_k - 1, y_k + 1)) \cdot \cos(45 + \alpha_k)$$

3. Normalization

In the normalization, iris region is transformed, so that it has fixed dimensions to allow comparisons between same iris images. The inconsistencies between same eye images are due to stretches of the iris caused by dilation of pupil from different illumination. Among other factors that cause dilation are: eye rotation, camera rotation, head tilt and varying image distance. The good normalization process must produce different iris regions for different iris, in the same condition and it must produce constant dimensions for the same iris in different condition. Another great challenge is that the pupil region is not always concentric within the iris region, and is usually slightly nasal (Daugman 2002). Daugman's rubber sheet model explains remap of each iris region's point to the polar coordinates (r,θ). r is moved in distance [0, 1] and θ is moved in angle [0, 2π].

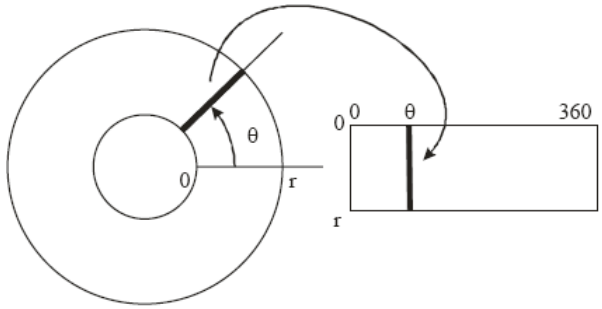

Figure 5. Daugman's rubber sheet model

The remapping of the iris region from (x, y) Cartesian coordinates to the normalized non-concentric polar representation is modeled as

$$I(x(r,\theta), y(r,\theta)) \rightarrow I(r,\theta)$$

With

$$x(r,\theta) = (1-r)x_p(\theta) + rx_I(\theta)$$
$$y(r,\theta) = (1-r)y_p(\theta) + ry_I(\theta)$$

The coordinates of the pupil and iris boundaries along the θ direction are xp, yp and xl, yl. The rubber sheet model is useful for accounting pupil dilation and size inconsistencies. This model however does not compensate for rotational inconsistencies.

Two iris templates are aligned with matching in shifting the iris templates in the θ direction to solve this problem.

3.1. Algorithm

Our algorithm on normalization of iris regions is based on Daugman's rubber sheet model (Daugman, et al. 2006). Since the pupil can be non-concentric to the iris, a remapping formula is needed to rescale points depending on the angle around the circle. This is given by

$$r' = \sqrt{\alpha}\beta \pm \sqrt{\alpha\beta^2 - \alpha - r_I^2}$$

With

$$\alpha = o_x^2 + o_y^2$$
$$\beta = \cos\left(\pi - arcton\left(\frac{o_y}{o_x}\right) - \theta\right)$$

The displacement of the centre of the pupil relative to the centre of the iris is given by oy, ox. The distance between the edge of pupil and the edge of iris at an angle θ is r' and the radius of the iris is rI. In order to prevent non-iris region data from corrupting the normalized representation, data points which occur along the pupil border or the iris border are discarded same as Daugman's rubber sheet model.

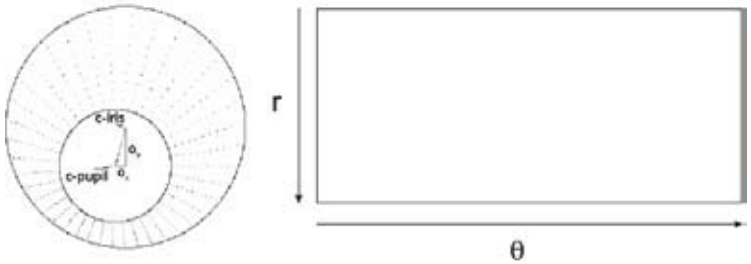

Figure 6. Outline of the normalization process with radial resolution of 10 pixels, and angular resolution of 40 pixels. Pupil displacement relative to the iris centre is exaggerated for illustration purposes

4. Result

Two standard iris databases have been selected for preliminary result. CASIA and MMU iris database are employed for testing the implemented algorithms. A brief statement of these databases will be presented in next sections.

CASIA Iris Database - CASIA-IrisV3 includes three subsets which are labeled as CASIA-IrisV3-Interval, CASIAIrisV3-Lamp, CASIA-IrisV3-Twins. CASIA-IrisV3 contains a total of 22,051 iris images from more than 700 subjects. All iris images are 8 bit gray-level JPEG files, collected under near infrared illumination. Almost all subjects are Chinese except a few in CASIA-IrisV3-Interval. Because the three data sets were collected in different times, only CASIA-IrisV3-Interval and CASIA-IrisV3-Lamp have a small overlap in subjects. CASIAIrisV3-Interval is a superset of CASIA V1.0 which has been requested by and released to more than 1,500 researchers/teams from 70 countries and regions (as of June 2006). CASIA V1.0 contains 756 iris images from 108 subjects. Both CASIA-IrisV3-Lamp and CASIA-IrisV3-Twins was collected using OKI's hand-held iris sensor. A lamp was turned on/off close to the subject to introduce more intra-class variations when we collected CASIAIrisV3-Lamp. CASIA-IrisV3-Twins contains iris images from 100 pairs of twins.

MMU Iris Database -MMU iris database contributes a total number of 450 iris images which were taken using LG IrisAccess®2200. This camera is semi-automated and it operates at the range of 7-25 cm. On the other hand, MMU2 iris database consists of 995 iris images. The iris images are collected using Panasonic BM-ET100US Authenticam and its operating range is even farther with a distance of 47-53 cm away from the user. These iris images are contributed by 100 volunteers with different age and nationality. They come from Asia, Middle East, Africa and Europe. Each of them contributes 5 iris images for each eye. There are 5 left eye iris images which are excluded from the database due to cataract disease.

The above algorithm is implemented with Delphi programming language. It is tested using CASIA and MMU database. In this case, more than 100 irises are randomly selected among of above databases. During detecting iris by this algorithm, most important thing is setting correct parameters. There are four parameters in the algorithm:

1. Smoothing Factor: This parameter is used in accumulating stage and indicates the width of binning square.
2. Smoothing Stage: It means that how many times the algorithm should accumulate the original image.
3. Suggest Radius: The radius of pupil in last binned stage.
4. Circle Sample: The number of points taken in to integration over the circle.

We have tested the algorithm in three different phases. In first phase all parameters are fixed for all images. We use Smoothing Factor = 3, Binning Stage = 4, Suggest Radius = 1 and Circle Sample = 64. The results are summarized in table.1.

Iris Database	Percentage of Correctness		
	Correct Detect	Correct Pupil or Correct Iris	Wrong Detect
CASIA	73	16	11
MMU Iris Database	77	14	9

Table 1. Execution Result with Fixed Parameters

In this phase, we see that, wrong detections could be corrected by changing the parameters. For example, as you can see in Figure 7, the iris didn't detected correctly in left image, but by changing smoothing factor to 5, it has been reclaimed (see right image).

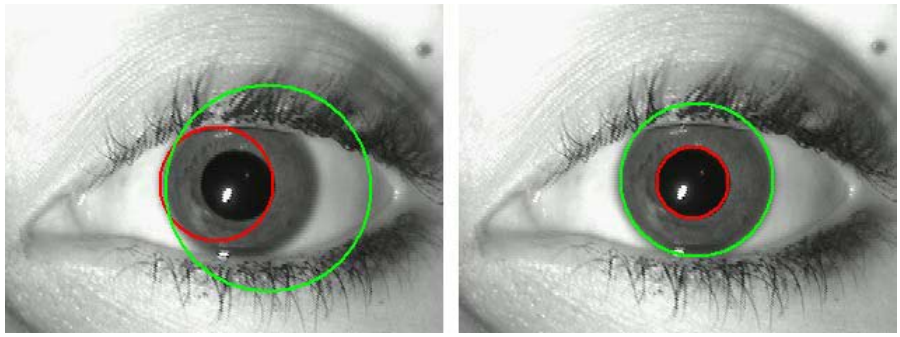

Figure 7. Left – Wrong Detection, Right – Reclaim by changing parameters

In the second phase, we try to change parameters for wrong detections and test again to obtain a better result. By default we set the parameters similar as before, however in wrong detection we adjust the parameters until it is correctly detected. The results of second phase are shown in Table.2.

Iris Database	Percentage of Correctness		
	Correct Detect	Correct Pupil or Correct Iris	Wrong Detect
CASIA	91	8	1
MMU Iris Database	94	5	1

Table 2. Execution Result with nonFixed Parameters

It is observed that the results are significantly improved, but still there is some incorrect detection. In some cases, the pupil can be correctly detected, conversely incorrect detecting the pupil. After adjusting the value of the parameter, pupil is wrongly detected. In the third phase, different parameter values are adopted to improve the detection rate. The results of the third phase are summarized in Table.III. The final detection of some iris images is depicted in Figure 8.

Iris Database	Percentage of Correctness	
	Detected	UnDetected
CASIA	98	2
MMU Iris Database	99	1

Table 3. Execution Result with Separate Parameters

The normalization process proved to be successful and some results are shown in Figure 9. However, the normalization process

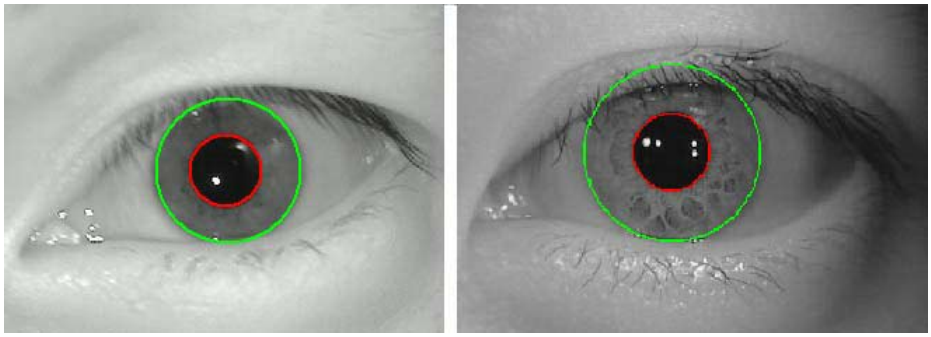

Figure 8. Rightly Detected Iris a)MMU - b)CASIA

is unable to perfectly reconstruct the same pattern from images with varying amounts of pupil dilation, since deformation of the iris results in small changes of its surface patterns.

Normalization of two eye images of the same iris is shown in Figure 9. The pupil is smaller in the bottom image, however the normalization process is able to rescale the iris region so that it has constant dimension. In this example, the rectangular representation is constructed from (360 * (Iris Radius – Pupil Radius)) data points in each iris region. Note that rotational inconsistencies have not been accounted for by the normalization process, and the two normalized patterns are slightly misaligned in the horizontal (angular) direction. Rotational inconsistencies will be accounted for in the matching stage.

5. Discussion and Conclusion

As we have shown in the previous section, the critical step of the algorithm is setting the correct parameters. By using fixed parameters values, the algorithm automatically detects both the iris and the pupil. However, the rate of correct detection is low and it is not acceptable. Conversely by allowing manual intervention of parameters setting by the user for wrong detec-

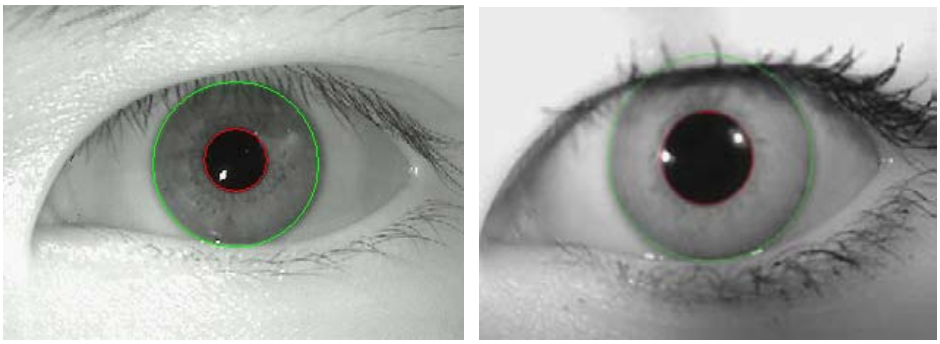

Figure 9. Illustration of the normalisation process for two images of the same iris taken under varying conditions

tion, the accuracy rate increases as shown in Figure 10.

As shown in Figure 11, with a high quality images, auto detection produces encouraging results. On the other hand poor iris images need user-intervention to increase the rate of correct iris and pupil detection. The poor image quality is due to the presence of shadow especially in corners that contribute to the wrong detection of center point. Another potential problem is associated with luminosity in some images that hinder the detection process. Further problem is due to the irregular image dimension. To overcome the above problems, we can either use more than one images or incorporating an intelligent technique to automatically adjust the associated parameters for correct detection. Another challenging problem that we encounter during the normalization stage is the effect of eye lashes towards the iris. We do not have to perform the noise removal if both iris and eye lashes have similar colors. Noise here is indicated by the presence of eye lashes. However, we need to remove the noise from the iris, if iris and eye lashes have different colors. The noise will affect the accuracy of a template generated from a normalized iris in our next venture.

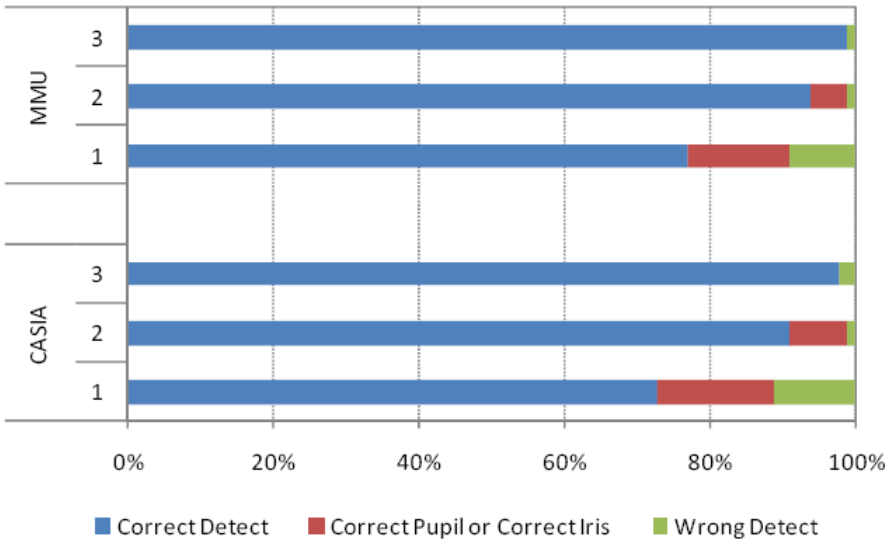

Figure 10. Percentage of Accuracy in Three Phases

5.1. Future Work

Some suggestion will be introduced to improve the proposed algorithm.

- Deleting the Number of Stages Parameter N
  - o This can be possible by employing a threshold for the size of last shrunk image. We continue the shrinking until the size of image will be less than threshold, for example 10 pixel.

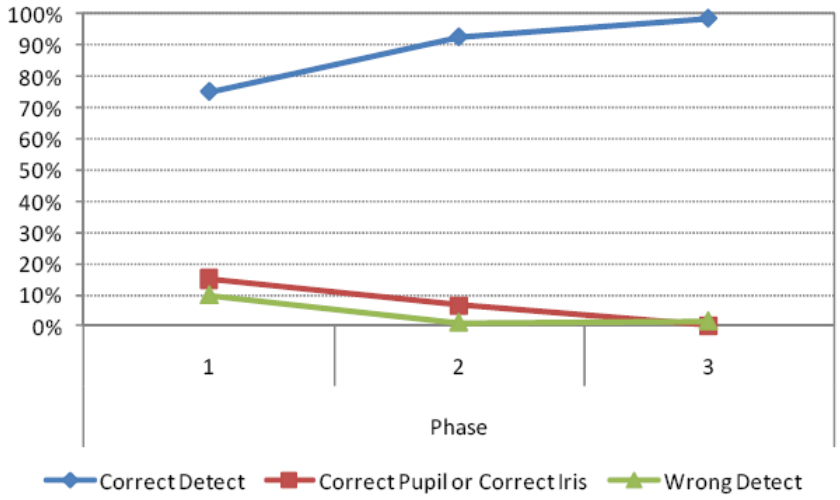

Figure 11. Final Success and Error Rate and Auto Detectability

- Also this improvement could help us to delete the range of radius parameter, because the investigation on the structure of the eye shows that the radius can be estimated about 2 pixels on the eye image with width of 10 pixels. The Iris size related to eye size is like 4 to 10.

- Improving the difference function
  - To apply a good high contrast method for increasing the contrast of image around the circle contour to find circle more accurately
  - To apply edge detection method similar to Hough transforms (Kong and Zhang 2001; Ma, Wang and Tan 2002; Tisse, Martin, Torres and Robert 2002; Wildes 1997).

References

[1] CASIA iris image database. In: http://www.sinobiometrics.com, vol. Chinese Academy of Sciences Institute of Automation,
[2] Barry C, N. R Database of 120 Greyscale Eye Images. Lions Eye Institute, Perth Western Australia
[3] Daugman JG (2002) How iris recognition works. Proceedings of 2002 International Conference on Image Processing
[4] Daugman JG, Anderson R, Hao F (2006) Combining Crypto with Biometrics Effectively. IEEE TRANSACTIONS ON COMPUTERS 55(9)
[5] Kong W, Zhang D (2001) Accurate iris segmentation based on novel reflection and eyelash detection model. Proceedings of 2001 International Symposium on Intelligent Multimedia, Video and Speech Processing, Hong Kong
[6] Kovesi P MATLAB Functions for Computer Vision and Image Analysis. In, vol.,
[7] Ma L, Wang Y, Tan T (2002) Iris recognition using circular symmetric filters. National Laboratory of Pattern Recognition, Institute of Automation, Chinese Academy of Sciences
[8] Mazur J (2007) Fast Algorithm for Iris Detection. Advances in Biometrics:858-867
[9] Ritter N (1999) Location of the pupil-iris border in slit-lamp images of the cornea. Proceedings of the International Conference on Image Analysis and Processing
[10] Sanderson S, Erbetta J (2000) Authentication for secure environments based on iris scanning technology. IEE Colloquium on Visual Biometrics
[11] Tisse C, Martin L, Torres L, Robert M (2002) Person identification technique using human iris recognition. International Conference on Vision Interface, Canada
[12] Wildes R (1997) Iris recognition: an emerging biometric technology. Proceedings of the IEEE 85(9)
[13] Wildes R, Asmuth J, Green G, Hsu S (2004) A system for automated iris recognition. Proceedings IEEE Workshop on Applications of Computer Vision
[14] Williams GO (2001) Iris recognition technology. Iridian technologies, Tech.Rep

[15] Wolff E (1976) Anatomy of the Eye and Orbit. 7th edition. Lewis H. K. & LTD Co.
[16] Oppenheim A., Lim J. (1981) The importance of phase in signals. Proceedings of the IEEE 69, 529-541
[17] Field D. (1987) Relations between the statistics of natural images and the response properties of cortical cells. Journal of the Optical Society of America
[18] http://www.cbsr.ia.ac.cn/IrisDatabase.htm
[19] http://www.oki.com/en/press/2006/z0611e.htm

Author Biographies

Mahboubeh Shamsi is a Lecturer of Computer Science at Islamic Azad University, Bardsir, Iran. She is also a Ph.D. candidate at University of Technology, Malaysia. She has Master's degrees in Computer Science from Islamic Azad University, Najafabad, Iran and a Bachelor's degree in Applied Mathematics from Isfahan University, Iran. Her research interests include Security, Image Processing, Biometrics, Handwriting recognition, and Mathematic.

Puteh Saad is an Associate Professor of Computer Science at University of Technology, Malaysia. She has a Ph.D. in Computer Science from University of Technology, Malaysia. She has Master's degrees in Computer Science from University of Strathclyde, UK. She has Bachelor's degrees in Chemistry from University of Malaya, and an Adv Diploma's degree in Computer Science from University of Technology, Malaysia. Prior to joining UTM he was Deputy Dean/Lecturer of School of Computer & Communication Engineering at The UniMAP, Perlis, Malaysia. Her research interests include Image Processing, Software Engineering, Biometric, and Neural Networks.

Abdolreza rasouli Kenari is a Lecturer of Computer Science at Islamic Azad University, Bardsir, Iran. He is also a Ph.D. candidate at University of Technology, Malaysia. He has Master's degrees in Computer Science from Islamic Azad University, Najafabad, Iran and a Bachelor's degree in Mathematics from Isfahan University, Iran. His research interests include Cryptography, Security, Data Mining, Distributed Database, Web App, Image Processing, Algorithms, and Mathematic.

Soudeh Shadravan is an Associate Lecturer of Computer Science at Islamic Azad University, Bardsir, Iran. She is also a Ms.C. student at University of Technology, Malaysia. She has Bachelor's degrees from Islamic Azad University, Meybod, Iran and an Adv Diploma's degree from Islamic Azad University, Bardsir, Iran in Computer Science. Her research interests include Network, Logical Phase, and Graphic.